International Journal of Advance and Applied Research
www.ijaar.co.in
ISSN – 2347-7075 Impact Factor – 8.141
Peer Reviewed Bi-Monthly
Vol. 7 No. 5 January – February - 2026

NixCoxLaxFe2-xO4 Magnetic Mixed Metal Oxide Nanocatalyst: Synthesis Characterization and Application for One-Pot Synthesis of Octahydroquinazolinone

V. V. Chaudhari[1], K. S. Lohar[2] & D. R. Kulkarni[3]

Department of Chemistry, Shrikrishna Mahavidyalaya Gunjoti, Dharashiv 4136.6(MS), India

DOI - 10.5281/zenodo.18919491

Abstract:

Lanthanum doped nickel-cobalt nano ferrites with chemical formula Ni0.5Co0.5Fe2-xLaxO4(0.00,0.25,0.50,0.75,0.1) were prepared using a simple sol gel auto combustion method. The XRD pattern confirms single phase cubic spinel structure. Lattice constant increase as increase in La+3 ion conent.X-ray density increases whereas bulk density decreases. Infrared spectroscopy of synthesis sample shows absorption bands 'v2' around 400 cm-1 and 'v1' at 600 cm-1 are allocated to the intrinsic stretching vibrations of octahedral and tetrahedral complexes respectively. The EDAX pattern confirms stoichiometric composition of element of synthesized ferrite nano particles. Scanning electron microscopy was applied to study the surface characteristics and uniform distribution of particle size and also prepared samples are porous in nature. Transmission electron microscopy carried out to know the particles size of synthesized ferrite samples and selected area electron diffraction pattern clearly shows that particle were well crystalline in nature. Magnetic measurements of ferrite nanoparticles were done by vibrating sample magnetometer(VSM). Nano spinel nickel-cobalt lanthanide ferrite nanoparticles is a easily synthesized, non-toxic, less expensive, effortlessly magnetically recoverable and green catalyst for the synthesis of octahydroquinazolinone derivatives through the condensation of dimedone and aromatic aldehyde with urea or thiourea.

Keywords: Lanthanum doped nickel-cobalt ferrites, Lattice constant, octahydroquinazolinone.

Introduction:

A multicomponent reaction (MCR) is a reaction that produces a product in a single step by combining three or more reactants in a single pot [1]. One of the most basic processes in organic chemistry is the creation of a new carbon-carbon bond. Compared to sequential synthesis, this results in extremely minimal waste or undesired by-product creation. MCRs are becoming more popular in organic synthesis because to their atom economy, ease of use, and typically exceptional output [2]. The formation of a new carbon-carbon bond is one of the most fundamental processes in organic chemistry. This produces very little waste or unwanted by-product generation when compared to sequential synthesis. MCRs are gaining popularity in organic synthesis due to their atom economy, usability, and generally excellent results [3]. MCRs enable the assembly of complicated compounds in a single pot, in contrast to the traditional sequential synthesis method. In contrast to the typical multi-step synthetic method of creating specific bonds in the target molecule, the defining The intrinsic ability of MCRs to generate many bonds in a single operation without isolating the intermediates, altering the reaction conditions, or introducing additional reagents is one of their characteristics.

These environmentally friendly methods are an effective means of producing biologically active compounds and streamlining procedures in the pharmaceutical sector [4]. Despite being widely recognized for more than a century, the

MCR concept for the synthesis of various organic structures has only lately begun to receive more attention [5] Multicomponent reactions serve as affective instrument in the arsenal of sustainable organic synthesis its collaborative use with additional green chemistry principles would bring organic chemists closer to the ideal synthesis [6]. In various multicomponent organic reactions, the required catalysts must possess the characteristics of many active sites, nanoscale dimensions, and an extensive surface area [7]. Ferrites are chemical compounds, ceramic with iron (III) oxide Fe2O3 as their principal components [8]. Many ferrites are spinel's with the formula AB2O4, where A and B represent various metal cations, usually including iron.

Spinel ferrites usually adopt a crystal motif consisting of cubic close-packed (fcc) oxides (O2−) with A cations occupying one eighth of the tetrahedral holes and B cations occupying half of the octahedral holes-that is, the inverse spinel structure. Spinel ferrite nanoparticles have attracted much attention because of their electronic, magnetic, and catalytic properties, all of which are different from those of their bulk counterparts. Among spinel ferrites, cobalt ferrite (CoFe2O4) has an inverse spinel structure in which, in the ideal state, all Co2+ ions are in B sites, and Fe3+ ions are equally distributed between A and B sites [9]. The catalytic activity and surface characteristics of ferrospinels ofnickel, cobalt, copper and their sulfate variants are synthesized through gentle chemical techniques at the coprecipitation method at room temperature to produce samples with large surface areas [10].

The application of ferrite nanoparticles as catalysts in organic reactions has gained interest. Significant interest in recent years. While employing a catalyst at the nanometer scale could attain a significant improvement in its catalytic performance, the key challenge for environmentally friendly chemistry involves the development of novel technologies for the separation and recycling of catalysts to substitute traditional methods. In this regard, substantial focus has been directed towards the employing magnetic metal oxide nanoparticles as heterogeneous and readily recyclable catalysts for different organic reactions [11]. The catalytic effectiveness of ferrites for many such reactions arises because of the ease with which iron can exchange its oxidation state between 2^+ and 3^+. Another important attribute of these materials, from commercial standpoint, is their stability under extremely reducing conditions, which is due to the spinel structure. Thus the reduction of Fe^{+3} to Fe^{+2} takes place without altering these lattice configurations so that upon re-oxidation, the original state is 2 retained [12]. Unlike the spinel ferrites, the catalyst Fe2O3 diminishes in activity as it becomes diminished to FeO and metallic iron. Magnetite iron oxide nanoparticles as a catalyst are capable of can be readily isolated with the aid of an external magnet, leading to a straightforward catalyst separation without screening [12]. Iron oxides exhibit a strong level of chemical uniformity and do not dissolve in organic liquids. Lately, increased studies have been conducted on a magnetic catalyst. Currently, functionalized magnetite nanoparticles are utilized as efficient catalysts in various chemical processes involving the creation of α-amino nitriles [13]. 1,1-diacetates from aldehydes [14], 1,4-dihydropyridines [15] etc. For these uses of magnetic metal oxides as Heterogeneous catalysts possess significant surface area and available porosity as important characteristics. Nano catalysis aids in the creation of new catalysts that exhibit superior activity and enhanced selectivity. and great stability. Nano catalysts offer numerous benefits compared to traditional catalysts. Systems; nonetheless, the separation and extraction of these minuscule nano catalysts from

the reaction Blending is not simple. To address this problem, the application of magnetic nanoparticles has surfaced as an effective remedy; Their paramagnetic and insoluble properties allow for simple and effective separation of the catalysts. From the reaction solution using an external magnet [16]. Nano size spinel ferrites have been prepared by various techniques such as wet chemical co-precipitation sol–gel combustion, hydrothermal process, ball milling, the micro-emulsion, and oxalate precursor method [8, 17 20].

Octahydroquinazolinone derivatives possess a recognized moiety for leading medicinal purposes. Agents. They have been utilized for antimicrobial purposes [21] anti-inflammatory analgesic [22], and antiviral [23] etc. purposes.

The synthesis of octahydroquinazolinone derivatives through MCRs has become more popular due to its simple synthesis method, cost-effectiveness, and high selectivity [24] Bigenelli reactions preferably use β-diketone rather than open-chain dicarbonyl compounds to synthesize octahydroquinazolinone [27]. The synthesis of octahydroquinazolinone by one-pot three component reaction of aldehydes, dimedone and urea or thiourea using different catalysts or chemical agents, such as Conc. HCl [27], Conc. H2SO4 [28], trimethylsilyl chloride (TMCl) [29], and Lewis acids (La(OTf)3, L2O3, ZrCl4) [30, 31] are reported.

Nevertheless, numerous procedures face one or more drawbacks, including severe reaction parameters, extended reaction duration, low yields, utilization of dangerous and costly catalysts, highly acidic environments, and they also experience the development of numerous side items. Thus, the creation of sustainable, productive, and eco-friendly methodologies remain appealing and highly sought after.Recognizing the significance of octahydroquinazolinone derivatives, we have chosen to synthesize octahydroquinazolinone derivatives (4a-g) through a one-pot three-component synthesis involving dimedone(1), aromatic aldehyde (2) and thiourea (3) utilizing magnetically recoverable and reusable catalyst cobalt ferrite spinel (Scheme-1)

Experimental:

All chemicals used were of analytical grade with purity ≥99% and all the stock solution with distilled water. Ferric nitrate (Fe(NO3)2.6H2O, Citric acid (C6H8O7), Nickel nitrate(Ni(NO3)3.6H2O, Cobalt nitrate (Co(NO3)2.6H2O, Lanthanum nitrate (La(NO3)3.6H2O were used as the starting material. Reaction procedure was carried out in air atmosphere without the protection of inert gas. Calculated stoichiometry molar amount of lanthanum, Nickel, Cobalt and Ferric nitrates are added with distilled water and mixed thoroughly using a magnetic stirrer unit metallic nitrates are dissolved completely at RT to get a clear solution. The molar ratio of the metal nitrates to the citric acid was taken as 1:3. An aqueous solution of citric acid was mixed with metal nitrates solution, then ammonia solution was slowly added to adjust this PH at 7. The mixed solution was kept on to a hot plate with continuous stirring at 90^0C.During evaporation the solution become viscous and finally formed a very viscous brown gel. When finally, all water molecules were removed from the mixture, the viscous gel began frothing. After few minutes the gel automatically ignited and burn with glowing flints. The decomposition reaction would not stop before the whole citrate complex was consumed. The auto-combustion was completed within a minute, yielding the brown colored ashes termed as a precursor. Obtained voluminous product was well grinded to get magnetic oxide nano powder's obtained ash was sintered at 900^0C for minimum

4 hours to achieve higher rate of crystallization and finally grinded so the La^{+3} doped NiCoFe2O4 ferrite nano powders can be obtained.

Characterization:

The crystal structure was checked by means of X-ray diffraction(XRD) method using diffraction equipped with CuKα radiation (λ=1.5405). To observe the transition phase development of the precursor samples, thermos-gravimetric(TGA/DTA) analysis was carried out by Microstructure investigated by JEOL-JSM-5600-N Scanning Electron Microscope.FTIR spectra were recorded by Perkin-Elmer infrared spectrophotometer in the range of 4000-350 cm^{-1}.Magnetic measurement carried at room temperature using the vibrating sample magnetometer.^{1}H NMR spectra of representative derivatives were recorded on Bruker-Avance III HD NMR 500 MHz spectrometer.

Synthesis of octahydroquinazolinone Derivatives:

In a round-bottom flask with a 50 mL capacity, a solution of dimedone (1) (10 mmol), aromatic aldehydes (2) (10 mmol), and urea (3) (15 mmol) was dissolved in a solvent (15 mL ethanol + 10 mL distilled water). Magnesium ferrite catalysts (10 mol%) were then added, and the reaction mixture was heated under reflux. TLC was used to track the reaction's completion [solvent system Ethyl acetate: n-Hexane (3:7)].(Scheme-I).

The reaction mixture was removed and allowed to cool to ambient temperature after the catalyst was magnetically fixed at the flask's bottom using a powerful magnet. After that, the reaction mixture was filtered. Following a washing with a mixture of ethanol and water, the residue of Octahydroquinazolinone derivatives 4a–g was dried. Using ethanol as a solvent, recrystallization was used to purify the product. After that, the melting point was noted and the yield percentage was computed.

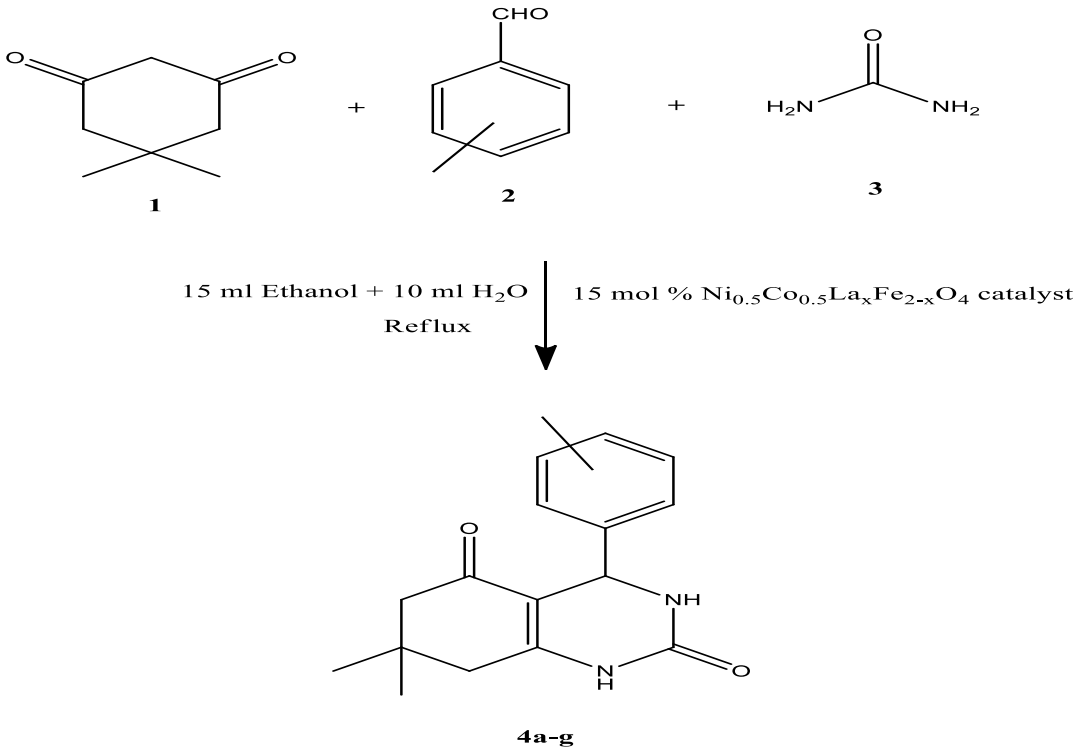

7,7-dimethyl-4-phenyl-4,6,7,8-tetrahydroquinazoline-2,5(1H,3H)-dione (4a):

m.p.192^{0}C,^{1}H NMR(500 MHzCDCl$_3$) δppm:1.11(s,3H,CMe);1.23(s,3H,CMe);2.42(m,2H,CH$_2$);2.42(m,2H,CH$_2$); 2.42(m,2H,CH$_2$);5.54(s,1H,CH);7.23(m,3H,Ar);8.12(d,2H,Ar);0.85(s,1H,NH);11.7(s,1H,NH).

4-(4-(dimethylamino)phenyl)-7,7-dimethyl-4,6,7,8-tetrahydroquinazoline-2,5(1H,3H)-dione (4b):

m.p.238^{0}C,^{1}H NMR(500 MHzCDCl$_3$) δppm:0.98(s,3H,NMe);0.98(s,3H,NMe);1.02(S,3H,CMe);1.12(s,3H,CMe);1.97(m,2H,CH$_2$); 2.33(m,2H,CH$_2$);4.66(s,1H,CH);7.16(d,2H,Ar);7.99(d,2H,Ar);10.47(s,1H,NH);10.47(s,1H,NH).

4-(2-hydroxyphenyl)-7,7-dimethyl-4,6,7,8-tetrahydroquinazoline-2,5(1H,3H)-dione (4c):

m.p.256^{0}C,^{1}H NMR(500 MHzCDCl$_3$) δppm:1.09(s,3H,CMe);1.21(s,3H,CMe);2.44(m,2H,CH$_2$);2.44(m,2H,CH$_2$); 5.47(s,1H,CH);7.01(m,2H,Ar);7.22(m,2H,Ar);11.51(s,1H,OH);11.56(s,1H,NH);11.86(s,1H,NH).

4-(4-hydroxy-3-methoxyphenyl)-7,7-dimethyl-4,6,7,8-tetrahydroquinazoline-2,5(1H,3H) dione (4d):

m.p.290^{0}C,^{1}H NMR(500 MHzCDCl$_3$) δppm:1.09(s,3H,CMe);1.22(s,3H,CMe);1.54(s,1H,OH); 2.38(m,2H,CH$_2$);2.38(m,2H,CH$_2$); 3.77(S,3H,OCH$_3$);5.48(s,1H,CH);6.8(d,H,Ar);6.81(d,H,Ar);7.00(d,h,Ar);11.67(s,1H,NH);11.9(s,1H,NH).

7,7-dimethyl-4-(4-nitrophenyl)-4,6,7,8-tetrahydroquinazoline-2,5(1H,3H)-dione (4e):

m.p.256^{0}C,^{1}H NMR(500 MHzCDCl$_3$) δppm:1.09(s,3H,CMe);1.2(s,3H,CMe);2.44(m,2H,CH$_2$);2.44(m,2H,CH$_2$);5.49(s,1H,CH);7.02(d,2H,Ar);7.26(m,2H,Ar);11.53(s,1H,NH);11.86(s,1H,NH).

4-(4-chlorophenyl)-7,7-dimethyl-4,6,7,8-tetrahydroquinazoline-2,5(1H,3H)-dione (4f):

m.p.260^{0}C,^{1}H NMR(500 MHzCDCl$_3$) δppm:1.11(s,3H,CMe);1.23(s,3H,CMe);2.23(m,2H,CH$_2$);2.23(m,2H,CH$_2$); 3.77(s,1H,CH);5.4(s,1H,NH);6.59(d,2H,Ar);6.81(d,2H,Ar);11.96(s,1H,NH).

4-(4-methoxyphenyl)-7,7-dimethyl-4,6,7,8-tetrahydroquinazoline-2,5(1H,3H)-dione (4g):

m.p.240^{0}C,^{1}H NMR(500 MHzCDCl$_3$) δppm:1.09(s,3H,CMe);1.22(s,3H,CMe);2.37(m,2H,CH$_2$);2.37(m,2H,CH$_2$); 2.89(m,2H,OCH$_3$);5.47(s,1H,CH);6.69(d,2H,Ar); 6.69(d,2H,Ar);11.66(s,1H,NH);11.93(s,1H,NH).

Results And Discussion:

XRD Analysis:

The XRD pattern of the calcinated $Ni_{0.5}Co_{0.5}La_xFe_{2-x}O_4$ ferrite sample is presented in fig.1.All the XRD peaks are characteristic of cubic spinel and no secondary peaks related to impurity phases observed in the XRD pattern[20].The observed XRD diffraction peaks were assigned to(220),(311),(222),(400),(422),(511),(440),(533) planes of La spinel ferrite.The average crystalline size from the most intense (311) peak were calculated using XRD and debye-Scherrer formula[21],Which is found to 21.128nm.

The Lattice parameter ‘a’ was calculated by using XRD data the equation discussed elsewhere[21,22],a=d$\sqrt{N}$,where ‘a’ is lattice parameter,’d’ is the initer planar spacing and $\sqrt{N} = \sqrt{(h2+k^2+I^2)}$.The calculated value of lattice parameter of La ferrite is A=8.3622 A^0 shows that the sample is to be cubic spinel structure. X-ray density (dX), bulk density (dB), porosity (P), and specific surface area (S) and hopping lengths (LA and LB) for the prepared nanoparticles is given in Table 1.

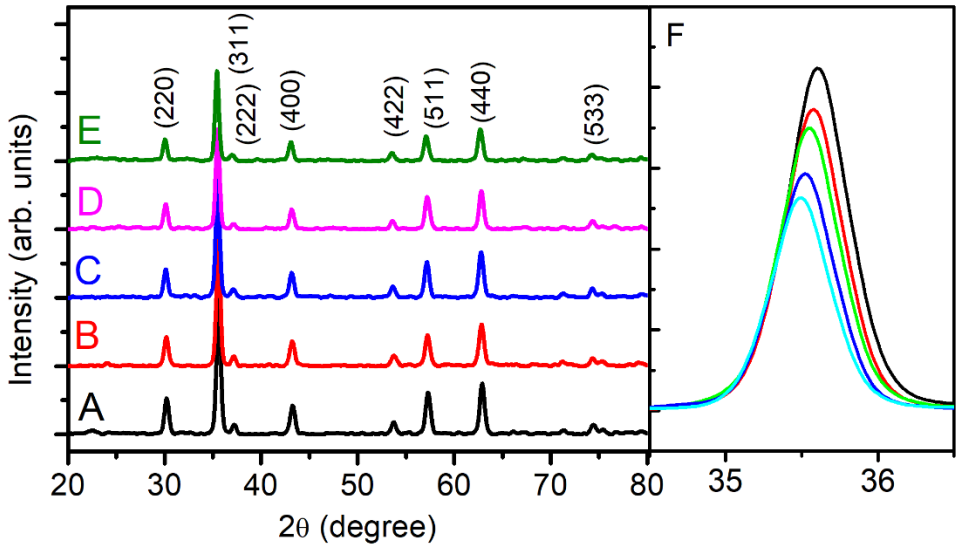

Fig. 1: XRD patterns (right panel) of $Ni_{0.5}Co_{0.5}Fe_{2-x}La_xO_4$ (where A: x=0.0, B: x=0.025, C: X=0.05, D: X=0.075 E: X=0.1) and (F) the expanded view of (311) peak (right panel).

Table 1: Lattice parameter (a), crystallite size (t), X-ray density (d_X), bulk density (d_B), porosity (P), and specific surface area (S) and hopping lengths (L_A and L_B) for the series $Ni_{0.5}Co_{0.5}Fe_{2-x}La_xO_4$.

'x'	'a' (Å)	't' (nm)	'd_X' (gm/cc)	'd_B' (gm/cc)	'P' (%)	'S' (m^2/gm)	L_A (Å)	L_B (Å)
0.0	8.3584	17.80	5.335	4.827	9.51	70	3.6193	2.9551
0.025	8.3603	19.96	5.379	4.841	10.00	62	3.6201	2.9558
0.050	8.3624	21.06	5.421	4.798	11.49	59	3.6210	2.9566
0.075	8.3641	22.24	5.465	4.762	12.87	57	3.6218	2.9572
0.1	8.3660	24.63	5.509	4.651	15.57	52	3.6226	2.9578

FTIR Analysis:

Fig.2.Show the FTIR spectra of the investigation $Ni_{0.5}Co_{0.5}La_xFe_{2-x}O_4$ nanocrystalline samples at increasing La^{3+} concentration. FTIR spectra demonstrate the presence of two fundamental absorption bands which are attributed to the normal and inverse cubic spinel ferrites. Generally the higher frequency absorption band 'ν_1' appears in the range of 500 to 570 cm^{-1} represents the intrinsic vibration of tetrahedral group, while the octahedral groups are represented by the lower frequency absorption band 'ν_2'in the range of 370 to 390 cm^{-1}[23,24].The characteristic bands that appear at wavenumber 540.25 cm^{-1} attributed to the metal-oxygen stretching vibration of Fe^{3+}-O^2 [25].Further the spectrum shows absorption bands at 1636.31 cm^{-1} presence of carboxyl group(COO-)[26].The difference in intensity of'ν_1' and 'ν_2' absorption bands is due to the changes in the bond length of Fe^{3+}-O^2 at tetrahedral A-sites and Octahedral B-sites[27].

Table 2:IR absorption bands of $Ni_{0.5}Co_{0.5}La_xFe_{2-x}O_4$

Comp.x	ν_1 (cm^{-1})	ν_2 (cm^{-1})
0.0	541.99	364.54
0.025	553.57	368.40
0.050	555.49	370.41
0.075	561.28	374.19
0.1	565.24	378.26

FESEM Analysis:

Scanning electron microscopy (SEM) of prepared nanoparticles was performed in order to ascertain in the surface morphology. From the images obtained it was found that each composition is characterized by a typical porous structure, which indicates the apparent changes in surface morphology was directly affected by variation in La ferrite substitution. It can be observed with increase in La ferrite substitution there is increase in porosity (Table No 1). The change observed in size of grain suggest that the inclusion of La in solution of solid takes place during preparation which leads to a better homogeneity in the powder and thereby a better controlled microstructure. It was observed from the SEM image that the prepared samples are porous in nature as shown in figure.3

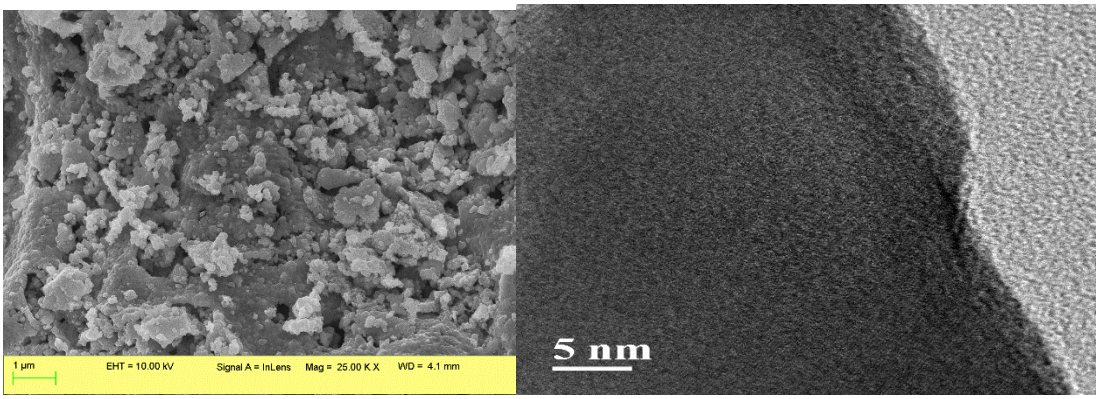

figure.3.SEM and TEM micrographs of calcinated Ni0.5Co0.5LaxFe2-xO4

EDX Analysis:

The elemental composition ,atomic percentage and their proportion were investigated by Energy dispersive analysis X-ray (EDAX) of La Substitutes Fe ferrite Ni0.5Co0.5LaxFe2-xO4 EDAX spectra of typical samples for of ferrite are shown in Figure.4 and Table No.3 From the figure the peaks of elements like Ni^{2+},Co^{2+},Fe^{3+},La^{3+},O^{2-} in edax spectra are confirmed. The EDAX spectra obtained La Substituted Fe ferrite indicate the presence of Ni in between the energy range of 7.5 keV and 8.4 keV,Co in the between the energy range 0.15 ke V and 6.5 ke V La in between 0.15 keV and 4.9 keV .The Fe was seen between 0.15 keV and 6.5 kev and Oxygen(O) was seen at 0.15 keV.

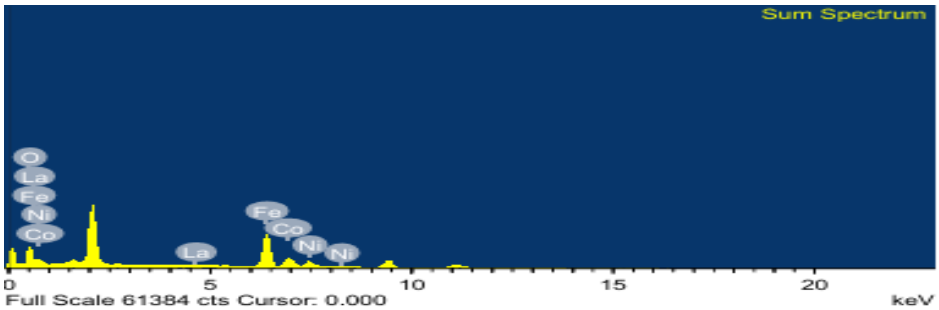

Table 3: EDX data of Ni0.5Co0.5LaxFe2-xO4

Comp.x		Ni	Co	La	Fe	O
0	Weight (%)	10.48	6.57	0	55.92	24.03
	Atomic (%)	6.28	5.71	0	35.21	52.8
0.025	Weight (%)	12.73	12.61	1.38	49.61	23.67
	Atomic (%)	7.72	7.62	35	31.63	52.68
0.05	Weight (%)	13.91	14.46	2.28	40.26	29.08
	Atomic (%)	7.8	8.08	0.54	23.73	59.85

0.075	Weight (%)	10.9	11.13	4	44.58	29.38
	Atomic (%)	6.11	6.22	0.95	26.28	60.44
0.1	Weight (%)	12.54	11.78	4.78	41.55	29.34
	Atomic (%)	7.06	6.6	1.14	24.59	60.61

Transmission electron microscopy (TEM):

The shape, size and morphology of the particles were examined by direct observation via transmission electron microscopy. The TEM $Ni_{0.5}Co_{0.5}La_xFe_{2-x}O_4$.samples are given shown in Figure 5a. The observation reveal that the particles were well distributed with slight agglomeration due high reactivity of samples by the heat treatment and magnetic interaction between particles. The Bragg's rings were observed in the selected area electron diffraction (SAED) patterns of typical TEM $Ni_{0.5}Co_{0.5}La_xFe_{2-x}O_4$ (X=0.050) samples are given in figure.5b. The polycrystalline nature of the samples was confirmed by the superimposition of the bright spot with the Debye ring pattern which is in accordance with XRD.(X=0.050) typical samples particles size distribution shown in Figure.5c.(0.1) .Nanocrystalline particles were in the range of 115-5-50 nm,with the most abundant being 20-25 nm.

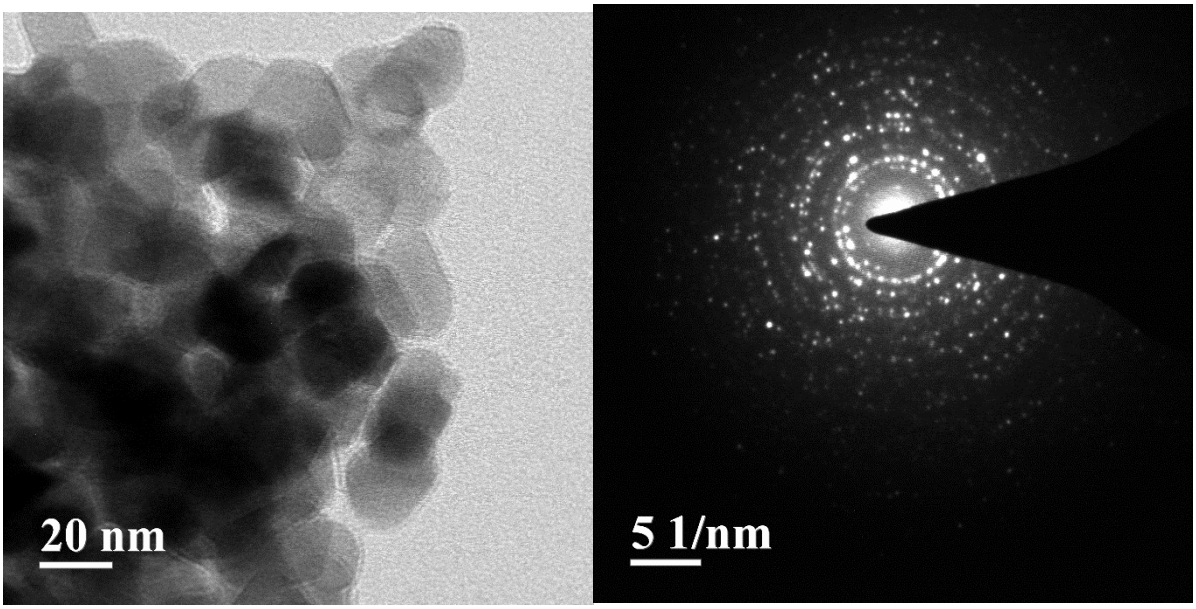

Optimum conditions for the synthesis of octahydrouinazolinone derivatives:

To begin with the quantity of nickel cobalt ferrite (catalyst load) became optimized for model reaction for compound **4a**,the use of benzaldehyde and urea. The catalyst was introduction in different quantities of 0,5,10,15 and 20 mol%.The results suggest that there is a positive correlation between the concentration of catalyst, ranging from 0 mol% to 15 mol% and the yield of the process. In the absence of catalyst (0 mol%) in model reaction 4a,the highest yields of 15% was obtained after a reaction time of 40 min (Table-1)

Table 1: Optimization of reaction conditions and catalyst load (mol %) of $NiCoLaFe_2O_4$ nanoparticles for the synthesis of of octahydroquinazolinone (4a).

Entry	Catalyst loading (mol %)	Time (min)	Yield of **4a**, [a] %
1	0	215	27:00
2	05	55	89.65
3	10	50	95.45
4	15	40	98.02
5	20	45	93.50

Conclusion:

In this work a non-toxic, low-cost, easily magnetically recoverable and green catalyst spinel nickel cobalt ferrite nanoparticles were efficiently synthesized by sol gel method. The XRD patterns and IR spectrum the formation of single phase cubic spinel nickel cobalt ferrite. A very fine spherical $NiCoLaFe_2O_4$ particles with some quantity of aggregation was observed within the SEM and TEM images. Octahydouinazolinone derivatives(4a-n) were efficiently synthesized using $NiCoLaFe_2O_4$ magnetic nanoparticles as heterogeneous catalyst with good yields and in short time.

Conflicts of Interest:

There are no conflicts to declare.

References:

1. Su, M., Liao, C., Lee, P. H., Li, H., & Shih, K. (2017). Formation and leaching behavior of ferrite spinel for cadmium stabilization. Chemical Engineering Science, 158, 287-293.
2. Gadkari, A. B., Shinde, T. J., & Vasambekar, P. N. (2010). Ferrite gas sensors. IEEE Sensors journal, 11(4), 849-861.
3. Naseri, M. (2015). Optical and magnetic properties of monophasic cadmium ferrite (CdFe2O4) nanostructure prepared by thermal treatment method. Journal of magnetism and magnetic materials, 392, 107-113.
4. Reddy, C. V., Byon, C., Narendra, B., Baskar, D., Srinivas, G., Shim, J., & Vattikuti, S. P. (2015). Investigation of structural, thermal and magnetic properties of cadmium substituted cobalt ferrite nanoparticles. Superlattices and Microstructures, 82, 165-173.
5. Chithra, M., Anumol, C. N., Sahu, B., & Sahoo, S. C. (2016). Exchange spring like magnetic behavior in cobalt ferrite nanoparticles. Journal of Magnetism and Magnetic Materials, 401, 1-8.
6. Priya, A. S., Geetha, D., & Kavitha, N. (2019). Effect of Al substitution on the structural, electric and impedance behavior of cobalt ferrite. Vacuum, 160, 453-460.
7. Dippong, T., Levei, E. A., & Cadar, O. (2021). Recent advances in synthesis and applications of MFe2O4 (M= Co, Cu, Mn, Ni, Zn) nanoparticles. Nanomaterials, 11(6), 1560.
8. Sachdeva, G., Dhariwal, J., Vats, M., Rawat, V., Srivastava, M., & Srivastava, A. (2022). Oxide Nanoparticles in Heterogeneous Catalysis. In Heterogeneous Catalysis in Organic Transformations (pp. 15-50). CRC Press 17
9. Aswin, K., Logaiya, K., Sudhan, P. N., & Mansoor, S. S. (2012). An efficient one-pot synthesis of 1, 4-dihydropyridine derivatives through Hantzsch reaction catalysed by melamine trisulfonic acid. Journal of Taibah University for Science,

6(1), 1-9.

10. Mariosi, F. R., Venturini, J., da Cas Viegas, A., & Bergmann, C. P. (2020). Lanthanum doped spinel cobalt ferrite (CoFe2O4) nanoparticles for environmental applications. Ceramics International, 46(3), 2772-2779.
11. Jauhar, S., Kaur, J., Goyal, A., & Singhal, S. (2016). Tuning the properties of cobalt ferrite: a road towards diverse applications. RSC advances, 6(100), 97694-97719.
12. Dias, F. D. S., Guarino, M. E. P., Pereira, A. L. C., Pedra, P. P., Bezerra, M. D. A., & Marchetti, S. G. (2019). Optimization of magnetic solid phase microextraction with CoFe2O4 nanoparticles unmodified for preconcentration of cadmium in environmental samples by flame atomic absorption spectrometry. Microchemical Journal, 146, 1095 1101.
13. Homayonfard, A., Miralinaghi, M., Shirazi, R. H. S. M., & Moniri, E. (2018). Efficient removal of cadmium (II) ions from aqueous solution by CoFe2O4/chitosan and NiFe2O4/chitosan composites as adsorbents. Water Science and Technology, 78(11), 2297-2307.
14. Ghorbani, H., Eshraghi, M., & Dodaran, A. S. (2022). Structural and magnetic properties of cobalt ferrite nanoparticles doped with cadmium. Physica B: Condensed Matter, 634, 413816.
15. Kharisov, B. I., Dias, H. R., & Kharissova, O. V. (2019). Mini-review: Ferrite nanoparticles in the catalysis. Arabian Journal of Chemistry, 12(7), 1234-1246.
16. Hayashi, Y. (2016). Pot economy and one-pot synthesis. Chemical science, 7(2), 866 880. 18
17. Sharma, S. D., Hazarika, P., & Konwar, D. (2008). A simple, green and one-pot four component synthesis of 1, 4-dihydropyridines and their aromatization. Catalysis Communications, 9(5), 709-714.
18. Maheswara, M., Siddaiah, V., Rao, Y. K., Tzeng, Y. M., & Sridhar, C. (2006). A simple and efficient one-pot synthesis of 1, 4-dihydropyridines using heterogeneous catalyst under solvent-free conditions. Journal of Molecular Catalysis A: Chemical, 260(1-2), 179-180.
19. Aldaghfag, S. A., Yaseen, M., Ambreen, H., Butt, M. K., Rehan, M., & Dahshan, A. (2021). Effect of Fe on physical characteristics investigations. Chalcogenide Letters, 18(7), 357-365. of CdS: DFT
20. Giribabu, G., Murali, G., Reddy, D. A., Liu, C., & Vijayalakshmi, R. P. (2013). Structural, optical and magnetic properties of Co doped CdS nanoparticles. Journal of alloys and compounds, 581, 363-368. 21. Tian, Y., Tao, Y., Huang, C., Geng, X., Gong, C., Wang, Z., ... & Yu, Z. (2023). Clusters of Fe–Co–Cd nanosheets grow on the surface of nickel foam to enhance the oxygen evolution reaction. Journal of Physics and Chemistry of Solids, 183, 111660.
21. Kumar, A., & Gangawane, K. M. (2022). Effect of precipitating agents on the magnetic and structural properties of the synthesized ferrimagnetic nanoparticles by co precipitation method. Powder Technology, 401, 117298.
22. Goldmann, S., Stoltefuss, J., & Elger, W. (1990). Structure-activity relationships of dihydropyridines with specific interaction at calcium channels. Journal of Medicinal Chemistry, 33(5), 1569-1575. https://doi.org/10.1021/jm00168a041
23. Triggle, D. J., Janis, R. A., & Goodnow, R. J. (2005). Development of the dihydropyridine class of calcium channel antagonists. Chemical Reviews, 105(8), 2497 2530. https://doi.org/10.1021/cr030100m 19
24. Gheorghe, C., Ciobanu, A., Radu, I., &

Uritu, C. M. (2021). 1,4-Dihydropyridines: Synthesis, properties, and applications. https://doi.org/10.3390/molecules26175248 Molecules, 26(17), 5248.

25. Elliott, H. L., & Ram, V. J. (2006). 1,4-Dihydropyridines and their therapeutic potential: An update. Current Medicinal https://doi.org/10.2174/092986706777934799 Chemistry, 13(16), 1937-1955.
26. Winkler, M., Peters, J., & Wolf, H. (1990). Structure-activity relationships of second generation dihydropyridines. Journal of Cardiovascular Pharmacology, 15(2), 345-352. https://doi.org/10.1097/00005344-199002000-00017
27. Bokštelė, R., Jarmalaitė, S., & Mickevičius, V. (2018). Synthesis and anticancer activity of 1,4-dihydropyridine derivatives. Bioorganic & Medicinal Chemistry Letters, 28(16), 2765-2771. https://doi.org/10.1016/j.bmcl.2018.06.057
28. Martin, A. C., Huerta, R., & Pichardo-Melendez, L. (2016). Antiviral properties of 1,4 dihydropyridines. International Journal of Antimicrobial Agents, 48(3), 284-289. https://doi.org/10.1016/j.ijantimicag.2016.05.016
29. Orrenius, S., Zhivotovsky, B., & Nicotera, P. (2003). Regulation of cell death: The calcium–apoptosis link. Nature Reviews Molecular Cell Biology, 4(7), 552-565. https://doi.org/10.1038/nrm1150
20.G.Allaedini,S.M.Tasirin and P.Aminayi,Int.Nano Lett.,5,183(2015);https://doi.org/10.1007/s40089-015-0153-8
30. Maddileti J,Vidyasagar T,Krishna Reddy C.V https://doi.org/10.1016/j.jre.2023.08.011-1002-0721/©20XX
31. B.L.Shinde,U.M.Mandle,A.m.Pachpinde and K.S.Lohar,J.Therm and Calorim,147,2947(2022);http://doi.org/10.1007/s10973-021-10719-0
32. Masoudpanah S, Ebrahimi SS, Derakhshani M, Mirkazemi S. Structure and magnetic properties of La substituted ZnFe2O4 nanoparticles synthesized by sol–gel autocombustion method. Journal of Magnetism and Magnetic Materials. 2014; 370:122–6.
33. Chaudhari V, Shirsath SE, Mane ML, Kadam RH, Shelke SB, Mane DR. Crystallographic, magnetic and electrical properties of Ni0.5Cu0.25Zn0.25LaxFe2−xO4 nanoparticles fabricated by sol–gel method. Journal of Alloys and Compounds. 2013; 549:213–20.
34. Ali I, Ahmad M, Islam M, Awan M. Substitution effects of La3+ ions on the structural and magnetic prop- erties of Co2Y hexaferrites synthesized by sol–gel autocombustion method. Journal of sol-gel science and technology. 2013; 68(1):141–9.
35. Awati V, Rathod S, Shirsath SE, Mane ML. Fabrication of Cu2+ substituted nanocrystalline Ni–Zn ferrite by solution combustion route: Investigations on structure, cation occupancy and magnetic behavior. Journal of Alloys and Compounds. 2013; 553:157–62.
36. Patil R, Delekar S, Mane D, Hankare P. Synthesis, structural and magnetic properties of different metal ion substituted nanocrystalline zinc ferrite. Results in Physics. 2013; 3:129–33.